Forest Ecology and Management 521 (2022) 120430

Contents lists available at ScienceDirect

Forest Ecology and Management

journal homepage: www.elsevier.com/locate/foreco

Intraseasonal interactive effects of successive typhoons characterize canopy damage of forests in Taiwan: A remote sensing-based assessment

Jonathan Peereman [a], J. Aaron Hogan [b,c], Teng-Chiu Lin [a,*]

[a] Department of Life Science, National Taiwan Normal University, No 88 Section 4, Ting-Chow Road, Taipei 11677, Taiwan
[b] Department of Biological Sciences, Florida International University, Miami, FL 33175, USA
[c] Department of Biology, University of Florida, Gainesville, FL 32611, USA

ARTICLE INFO

Keywords:
Vegetation index
Canopy disturbance
Residual effects
Successive tropical cyclones
Subtropical forests
Taiwan

ABSTRACT

Wind gusts and rainfall from tropical cyclones can heavily damage forest canopies, leading to abrupt changes in forest structure and tree demography. Although many studies have shown that successive tropical cyclones can interact with each other through residual effects, the role of past disturbances is unclear because they may lead to damage amplification of the second cyclone because of weakened forest structure, or damage reduction of the second cyclone because of previous damage to susceptible trees. We investigated the interaction between consecutive cyclones between 2001 and 2017 for five well-conserved forests in Taiwan, which experiences an average of 1.75 typhoons annually. Using MODIS imagery, we computed the typhoon-induced change of a canopy vegetation index, the Normalized Difference Infrared Index (NDII). The effects of successive typhoons were assessed separately for typhoons occurring within a single year (annual analysis) and within two consecutive years (biennial analysis). We used mixed effect models of reductions in NDII, a measurement of canopy damage, in relation to target and past typhoon characteristics and damage magnitude. NDII reduction induced by preceding typhoons was slightly more important and statistically significant in explaining the variation in NDII reduction associated with the target typhoon in the annual than in the biennial analysis, where the effect was non-significant. Canopy damage did not always decrease across typhoons occurring within the same season, however, for most successive typhoons in the biennial analysis, the second cyclone caused equal or less canopy damage (16 out of 21 typhoon pairs). These results support the idea that residual interactive effects of previous typhoons decrease quickly over time and rarely last for several typhoon seasons for Taiwanese forests, contributing to their high resistance to frequent typhoon disturbance.

1. Introduction

Tropical cyclones (known as typhoons in the Northwest Pacific and hurricanes in the North Atlantic) are major disturbances to forest ecosystems. Strong winds and high rainfall from cyclones damage trees. Tree damage ranges from defoliation and branch fall to stem breakage and whole-tree uprooting (Lugo, 2008; Mabry et al., 1998). In turn, these damages influence forest carbon fluxes and stocks through effects on forest biomass and litterfall production and decomposition (Liu et al., 2018; Uriarte et al., 2009; Wang et al., 2013; Xu et al., 2004) as well as alterations to forest structure (Brokaw and Grear, 1991; Flynn et al., 2010; Roth, 1992). Typically, taller trees are disproportionally damaged (Ostertag et al., 2005; Taylor et al., 2019 but see de Gouvenain and Silander, 2003) so that post-cyclone forests tend to be shorter and with more canopy gaps – caused by tree and branch falls – than they are in the absence of cyclone disturbance (Brokaw and Grear, 1991; Lagomasino et al., 2021; Li et al., 2021; Lin et al., 2020; Parker et al., 2018; Yamamoto, 2000).

Cyclone characteristics, such as wind speed, wind direction, and rainfall, can vary locally to modulate disturbance effects (Cortés-Ramos et al., 2020; Hogan et al., 2020; Peereman et al., 2022; Taillie et al., 2020). In addition, cyclone history should play a significant role in

Abbreviations: CI, confidence interval; IBTrACS, International Best Track Archive for Climate Stewardship; LAI, leaf area index; MAIAC, Multi-Angle Implementation of Atmospheric Correction; MODIS, MODerate resolution Imaging Spectroradiometer; NDII, Normalized Difference Infrared Index; NIR, near infrared; SWIR, shortwave infrared; VI, vegetation index.

* Corresponding author.
E-mail address: tclin@ntnu.edu.tw (T.-C. Lin).

https://doi.org/10.1016/j.foreco.2022.120430
Received 9 June 2022; Received in revised form 15 July 2022; Accepted 16 July 2022
Available online 26 July 2022

explaining cyclone canopy damage, due to the residual effects of the previous cyclones (Buma and Wessman, 2011; Johnstone et al., 2016). The legacy of a cyclone has an influence on the effect of later disturbances, given that post-cyclone forest canopy ingrowth of leaves and fine canopy branches generally takes several years, and coarser canopy branch ingrowth taking up to decades (Lin et al., 2017; Sharma et al., 2021). Hence, damage magnitude of subsequent cyclones likely varies with the time since the last disturbance.

Repeated cyclone disturbance over a short period can arrest the successional development of forests, maintaining early successional states (Janda et al., 2021; Uriarte et al., 2009). In tropical forests, temporally clustered cyclones over multiple years can result in severe and increasing forest damage, with each cyclone further damaging the forests, increasing debris deposition (*e.g.*, ground litter) and leading to shorter forests (Ibanez et al., 2019; Liu et al., 2018; Wang et al., 2013). For instance, four cyclones of category $\geq$ 2 (Saffir-Simpson scale; Simpson and Riehl, 1981) that passed over the Fiji Islands within eight years, led to the loss of > 75% of mangrove forests between 2001 and 2018 (Cameron et al., 2021). Moreover, forest demographic model simulations have shown cyclical storm occurrence preserves land-use legacies in secondary forest areas of hurricane-affected Puerto Rican forests by altering the size-distribution of adult trees (>10 cm dbh) and the recruitment response of the forest to canopy opening (Uriarte et al., 2009). Thus, cyclones occurring within the same season may lead to increased forest damage and novel forest recovery trajectories. For example, six typhoons passed over northern Taiwan in 1994 and led to an accumulated decrease in forest leaf area index (LAI) of about 66% (Mabry et al., 1998), and four typhoons that occurred in the 2008 typhoon season in Taiwan all caused significant leaf and branch fall in hardwood forests of central Taiwan (Wang et al., 2013). Yet, forest damage facilitation by previous cyclones on later disturbances ("linked disturbance", Simard et al., 2011) in these examples is unclear and it is challenging to distinguish the individual effects of all factors.

The damage pattern among consecutive cyclones can vary widely and the factors influencing variation need further investigation. In fact, observations of successive cyclones have shown that recent cyclone legacies can increase or decrease the damage severity caused by subsequent cyclones (Mabry et al., 1998; Ostertag et al., 2003; Ostertag et al., 2005). For example, in the Solomon Islands, the last cyclone of the four cyclones that occurred between 1967 and 1970 caused the most-severe damage (Burslem and Whitmore, 1999). Whether the severity in forest damage by the last cyclone is due to its characteristics (*e.g.*, wind speed, distance), or forest damage facilitation by previous cyclones is oftentimes unclear. The second of two cyclones might have been the most severe because it had the highest wind speed, or due to the effects of previous cyclones, or both. Damage facilitation originating from recent cyclones has been linked to factors such as cyclone's maximum wind speed and rainfall, as well as the type of recent tree damage. Indeed, damage facilitation can occur through tree weakening, either because of root damage or to the degradation of tree aboveground structure. For instance, trees damaged (snapped or uprooted) by Hurricane Hugo in 1989 were more likely to be damaged again by Hurricane Georges in 1998 (Ostertag et al., 2005). Mabry et al. (1998) reported similar relationships in Taiwan where trees partially uprooted or bole-snapped by a first typhoon had greater tip-up prevalence after a second typhoon occurring within the same cyclone season. Besides, heavy rain from cyclones affects soil and tree stability, thus increasing the chance of tree fall and the vulnerability of forests to later cyclones (Bellingham et al., 1992; Hall et al., 2020; Morimoto et al., 2021).

Conversely, a decrease in damage severity (*i.e.*, the opposite of damage facilitation) associated with subsequent cyclones has also been reported. In Puerto Rico, the 1998 Hurricane George caused less damage than the 1989 Hurricane Hugo (Ostertag et al., 2003). Higher wind speeds of Hurricane Hugo (category 4) than Hurricane George (category 3) certainly contributed to the greater damage associated with Hurricane Hugo than Hurricane George (Ostertag et al., 2003). However, less wind-exposed standing vegetation (*e.g.*, lower canopy height) following Hugo also played a role in less damage being attributed to George (Ostertag et al., 2003). In central Taiwan, the removal of a substantial proportion of the forest canopy by earlier typhoons has been suggested to contribute to decreased litterfall production and storm-induced litter deposition for subsequent cyclones within the same season (Wang et al., 2013). Although explanations have been proposed regarding how residual effects of recent cyclones may facilitate or decrease the damage of subsequent cyclones, it is difficult to generalize because we do not have enough studies to clearly distinguish the effects of multiple drivers (*e.g.*, wind speed, rainfall, site history) that affect residual effects independently or interactively. For instance, Parker et al. (2018) studied the effects of two hurricanes, a category 2 storm in 2011 and a category 5 storm in 2015, over the same region, however assessing the effect of the preceding hurricane legacies on the 2015 hurricane damages was complicated by differences in maximum wind speed between the two storms. In this case, the effects of the second and stronger storm were confounded with damage facilitation caused by the first hurricane. Therefore, comparing different scenarios of successive cyclones occurrence (*e.g.*, both stronger-then-weaker successive cyclones and weaker-then-stronger ones) within the same cyclone season or across multiple cyclone seasons, is necessary to have a more complete picture of the effects of recent past cyclones on later cyclone disturbances over the same region.

Remote sensing techniques are extensively used to monitor cyclone disturbances at the landscape scale (*e.g.*, Chambers et al., 2007; Feng et al., 2020; Peereman et al., 2022). Because approaches can be standardized, remote sensing data are useful for comparing multiple disturbance events over time and at various spatial scales. For instance, Wang et al. (2016) estimated litterfall dynamics in Taiwanese forests over 10 years using the Moderate Resolution Imaging Spectroradiometer (MODIS) data, and documented interannual variation that reflected typhoon canopy damage and recovery dynamics. Similarly, de Beurs et al. (2019) computed a MODIS-based disturbance index to monitor the effects of cyclone disturbance and drought and their interaction across Caribbean forests. However, that study did not investigate relationships between multiple cyclone events or residual effect over time. Many studies have relied on vegetation indices (VI) to monitor canopy change (Peereman et al., 2020; Rossi et al., 2013; Wang et al., 2010). Among the numerable VIs, the Normalized Difference Infrared Index (NDII, Hardisky et al., 1983) tracks canopy water content and can be used to assess canopy change dynamics. In fact, NDII has been shown to be a reliable proxy for forest canopy cover change (Gang et al., 2020; Jin and Sader, 2005; Wang et al., 2010).

Despite the large number of studies that have used remote sensing approaches (Frolking et al., 2009), few have endeavored to compare the effects of different cyclones over a same region (Cortés-Ramos et al., 2020; McLaren et al., 2019; Parker et al., 2018; Peereman et al., 2020). Little is known of the interaction between temporally clustered cyclones. Yet, a better understanding of how temporally clustered cyclones affect forests and the factors that modulate disturbance effects is critical because forests are likely to experience an increasing frequency of severe cyclone disturbances. Global climate change is expected to create larger and more-powerful cyclones (Sun et al., 2017) with slowing translation speeds and increased rainfall (Patricola and Wehner, 2018; Takemi, 2019; Zhang et al., 2020). Moreover, global climate change will continue to shift tropical cyclone trajectories toward coastal area (Wang and Toumi, 2021), with a higher frequency of landfalls in some regions such as in the North-Western Pacific (Liu and Chan, 2020; Xiao, 2021).

Due to its location within the North-Western Pacific cyclone hotspot, Taiwan has an extensive cyclone record to analyze the effects of recurring disturbances in relation to short cyclone return intervals, providing observations that are relevant for other regions where cyclones are expected to become more frequent. Although cyclones have long-lasting consequences on ecosystems (*e.g.*, Lin et al., 2017; Murphy et al., 2014), we focus our analyses on cyclones which have occurred within

the same cyclone season (annual) that generally spans from July through October, or within two consecutive cyclone seasons (biennial) because Taiwan is exposed to frequent cyclone disturbance. According to the International Best Track Archive for Climate Stewardship (IBTrACS), the frequency of ≥ category 1 typhoons passing within 100 km of the main island has averaged 1.75 typhoons per year from 1980 to 2020 (Knapp et al., 2018; Knapp et al., 2010). Using NDII, we quantify the effects of annual and biennial successive typhoons on canopy damage magnitude for five forests in Taiwan, accounting for current and past typhoon characteristics. We address the following questions:

i) What is the importance of recent past-typhoon legacy in explaining the canopy damage magnitude of subsequent typhoons?
ii) Is the relationship between two successive typhoons within a typhoon season maintained if they occurred within two successive typhoon seasons (*i.e.*, if cyclones are separated by a growing season)?
iii) Is the relationship between two successive typhoons modulated by the relative wind speed of the two typhoons (*i.e.*, different when the first typhoon had stronger versus weaker wind speeds than the second typhoon)?

We hypothesized that cyclone disturbance effects compound one another when occurring in rapid succession (*i.e.*, within the same season), and hence canopy damage caused by the first typhoon will facilitate canopy damage by subsequent typhoons. Furthermore, we anticipated that more damage should be caused by the second typhoon when the first typhoon had stronger wind speeds and more rainfall than the second typhoon, because it should have increased the vulnerability of the forest to canopy damage by the second typhoon.

2. Material and methods

2.1. Studied sites

Five montane forests across Taiwan were selected (Fig. 1; Fig. S1). The site selection was based on the following criteria: being located within a protected area and hence relatively free of direct anthropogenic influence, being large enough to accommodate coarse spatial resolution imagery (500 m, MODIS) and being located at different latitudes across the Central Mountain Range of Taiwan that spans the island along its North-South axis so that sites were representative of Taiwanese montane forests. Moreover, all sites except Lienhuachih (538 to 930 m) span considerable altitudinal ranges (228 to 1352 m for Chachaylaishan, 485 to 1451 m for Fushan, 296 to 1842 m for Lijia, 872 to 3450 m for Yuli). All sites are subject to very frequent typhoons, ranging from 26 to 31 typhoons ≥ category 1 and 11 to 15 typhoons ≥ category 3 passing within 100 km of each site centroid between 1980 and 2017 (IBTrACS). Given that the typhoon frequency is comparable across all sites, it is unlikely that differences in canopy resistance mediated by cyclone frequency have arisen differently among sites (Peereman et al., 2022).

2.2. Datasets

Studied areas were delineated using the Worldwide Database of Protected Areas (IUCN and UNEP-WCMC, 2021; for Chachayalaishan,

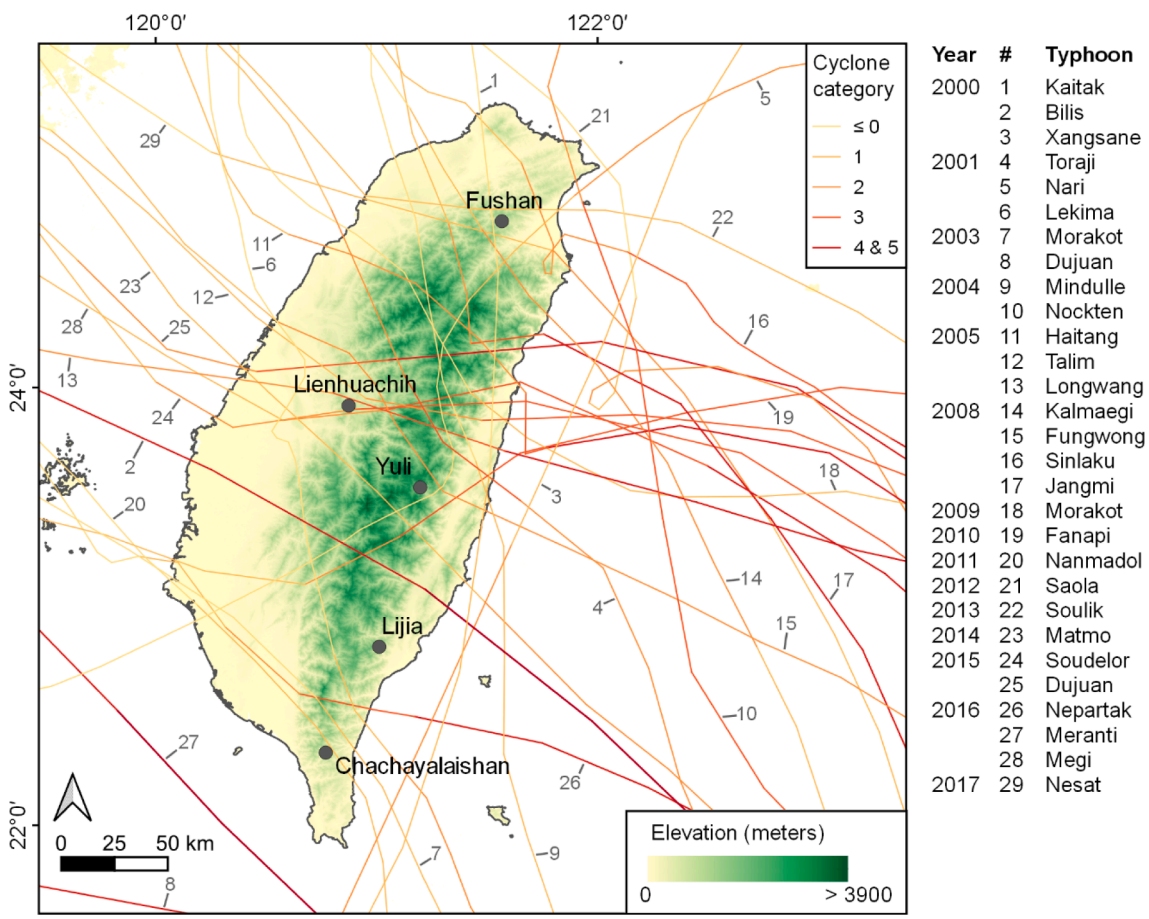

Fig. 1. Locations of the five Taiwanese forest sites and tracks of the 29 typhoons included in the study. Track colors indicate their intensity according to the Saffir-Simpson scale and IBTrACS dataset (Knapp et al., 2018; Knapp et al., 2010; Simpson and Riehl, 1981). Taiwan's central mountain range is shown in green based on the Aster global digital elevation model version 2. The five forest sites are shown in Supporting Information Figure S1. (For interpretation of the references to color in this figure legend, the reader is referred to the web version of this article.)

Lijia, Yuli) and personal knowledge of the forest areas (Dr. Chung-Te Chang, personal communication). The typhoon data were extracted from the IBTrACS dataset on world cyclone tracks. We selected all typhoons ≥ category 1 (wind speed ≥ 119 km/h) on the Saffir-Simpson scale within 100 km range from each site centroid which occurred within a two-season window.

To monitor forest canopies, we used the MODIS global daily ground reflectance data from NASA's Terra and Aqua satellites (MCD19A1 collection version 6) (Lyapustin and Wang, 2018). The MCD19A1 collection is a daily imagery product available for years after 1999 with a 500 m spatial resolution for bands 1 to 7 (blue to short-wave infrareds). The MCD19A1 collection is derived from the Multi-Angle Implementation of Atmospheric Correction (MAIAC) algorithm processing that allows for improved cloud detection and atmospheric and aerosol correction over time (Lyapustin et al., 2011a; Lyapustin and Wang, 2018; Lyapustin et al., 2011b). VI-based studies of evergreen tropical forests have used the MCD19A1 collection in the Amazon, Africa, and Southeast Asia (Hashimoto et al., 2021; Nunes et al., 2019; Ploton et al., 2020). Furthermore, although Landsat or Sentinel imagery have finer spatial resolutions, their lower temporal resolutions make the study of tropical and subtropical forests difficult because of frequent cloudiness (Asner, 2001; Negrón-Juárez et al., 2014b), including forests in Taiwan (Thies et al., 2015).

To constrain the analysis to areas without forest loss across the study period (*i.e.*, from 2001 to 2017), we used the MODIS collection MCD12Q1 version 6, which provides yearly-supervised land surface classification since 2001 at a 500 m resolution. The MCD12Q1 collection contains different classification schemes, among which we selected the one from the International Geosphere-Biosphere Programme. Table S1 in the Supplementary materials provides the list of MCD19A1 and MCD12Q1 scenes used in this study.

For each typhoon, we computed the pixelwise nearest distance to the typhoon track. In addition, we used the HURRECON model to estimate pixelwise maximum wind speed based on the IBTrACS dataset and the "HurreconR" package (Boose et al., 1994). The HURRECON model computes local maximum wind speed and wind direction based on the land cover and distance from the typhoon paths, however it does not take topography into account. Therefore, we computed the windwardness of each pixel as a measure of wind exposure, as windwardness has been shown to affect severity of typhoon disturbance (Boose et al., 2004). Windwardness is the angle between wind direction computed by HURRECON and the slope aspect (Feng et al., 2020). A windwardness of 0° implies that the pixel and the wind face the same direction (leeward) and the slope is not exposed, whereas an angle of 180° signifies that slope and wind face opposite directions and that the slope is thus exposed (windward).

2.3. Processing and vegetation indices

All MODIS-derived data were retrieved using the package "MODIStsp" (Busetto and Ranghetti, 2016) in R 4.0.3 (R Core Team, 2020), and re-projected to the 51 N UTM Zone (WGS-84) using bilinear (MCD19A1) and nearest neighbor interpolation (MCD12Q1).

We computed the NDII (equation (1)), a vegetation index based on the NIR and shortwave infrared (SWIR) band 7. MODIS sensors have three SWIR bands, centered on 1240 nm (band 5), 1640 nm (band 6) and 2130 nm (band 7) wavelengths. We selected band 7 over bands 5 and 6 because studies have shown that NDII based on bands 6 or 7 monitored canopy defoliation better than NDII based on band 5 (de Beurs and Townsend, 2008; Gao, 1996), and because band 6 of the Aqua sensor has striping issues (*i.e.*, periodic noise across the image; Wang et al., 2006). Being based on SWIR and NIR, NDII is used to track leaf water content (Ceccato et al., 2001). In addition, NDII has been extensively used to investigate cyclone disturbances on forest landscapes and is more sensitive than other VIs to canopy change, especially in high biomass forests (Gang et al., 2020; Jin and Sader, 2005; Wang et al., 2010; Zhang et al., 2016).

$$\mathrm{NDII} = \frac{\mathrm{NIR} - \mathrm{SWIR}}{\mathrm{NIR} + \mathrm{SWIR}} \tag{1}$$

Given the high cloudiness of Taiwan, all scenes (*i.e.*, images) 30-days before and after typhoon passage were considered; this period typically avoids early canopy recovery that begins within the first month after disturbance (using MODIS, de Beurs et al., 2019). Scenes within this period were merged to produce composite imagery, characterizing the forest canopy before and after disturbances. The maximum NDII values of each pixel were selected among all possible values because they describe the reflectance values of the canopy with minimal loss through the atmosphere. No further processing was applied given that the MAIAC algorithm provides surface reflectance data with identified cloudy pixels, which were excluded from the analysis.

To characterize the effect of successive typhoons, we computed the relative change in NDII values, ΔNDII (equation (2)), which is defined as the difference between pre- and post-typhoon NDII values divided by the pre-typhoon NDII value for each pixel. Hence, a positive value indicates that the canopy was damaged by the typhoon; the greater the value, the greater the canopy damage. We studied pairs of successive typhoons in two types of succession: typhoons that had occurred within the same typhoon season (*i.e.*, the annual analysis), and typhoons that had occurred within two consecutive typhoon seasons with typhoons being separate by a non-typhoon growing season (*i.e.*, the biennial analysis). Analyses were conducted independently to minimize the loss of pixels due to cloud cover. All values were then extracted using the "raster" package (Hijmans, 2019) after resampling of elevation, wind speed and windwardness products to the MODIS resolution using bilinear interpolation.

$$\Delta\mathrm{NDII} = \frac{\mathrm{NDII}_{\mathrm{pre-disturbance}} - \mathrm{NDII}_{\mathrm{post-disturbance}}}{\mathrm{NDII}_{\mathrm{pre-disturbance}}} \tag{2}$$

2.4. Data analyses

We removed outliers (values above and below first and third quartiles: ± 1.5 × inter quartile range) in NDII before computing ΔNDII (Tukey, 1977). Then, all ΔNDII < 0 were set to 0 as they do not describe loss of canopy; hence 0 indicates the absence of damage.

2.4.1. Role of typhoon characteristics and preceding disturbance

Pearson correlation analysis was used to assess the correlation between the windwardness of the target and preceding typhoons in both annual and biennial analyses in order to assess whether some areas is generally more exposed to typhoons.

We used linear mixed effects models of the canopy damage based on ΔNDII and predictors related to target typhoon characteristics, pre-typhoon vegetation conditions, and the NDII change caused by the preceding typhoon. A variable composed of site and typhoon identity was used as random intercept term (*e.g.*, 'lonlie' for Typhoon Longwang in Lienhuachih forest). Spatial correlation among sites was addressed using the pixel coordinates and an exponential structure in the model variance–covariance structure. First, multicollinearity among predictors was assessed by computing pairwise correlations, and for highly correlated predictor pairs ($r > 0.8$), the predictor with the lowest correlation with ΔNDII was excluded from models. For the annual analysis, predictor variables related to the target typhoon and the preceding typhoon were considered. Target typhoons variables were pixelwise maximum wind speed, and windwardness. We also included altitude (from ASTER GDEM V2) because the sites covered large elevation gradients. The preceding typhoon was characterized by the ΔNDII associated with its passage. The $\mathrm{NDII}_{\mathrm{pre\text{-}cyclone}}$ was also included because it characterizes the canopy state of the forest stand before the target typhoon event. ΔNDII was log-transformed to improve normality and all fixed predictors except for wind speed were scaled and centered for each event

(mean of 0 and standard deviation of 1). Wind speed could not be normalized because all pixels had the same values in some instance. The model was fitted using restricted maximum likelihood. Marginal and conditional model goodness of fit (R^2) are reported using the Nakagawa et al. (2017) method.

The linear mixed-effects model for the biennial analysis was fitted similarly, although predictors covered two separate years: the year of the target typhoon, and the typhoon season of the preceding year. For the biennial analysis, we used the same predictor variables as for the annual analysis, but for the typhoon of the target year, and for all typhoons in the previous typhoon season. We included the $NDII_{pre\text{-}cyclone}$ value, to represent the canopy state of the forest before disturbance. Total ΔNDII between the first and last typhoons was used to characterize the previous typhoon season, hence describing the effect of the previous typhoon season on the canopy.

2.4.2. Typhoon strength, and variation in damage severity between successive events

To assess whether the degree of canopy damage (*i.e.*, changes in NDII) caused by each target typhoon was different from the preceding event, we compared $\Delta NDII_{typhoon}$ and $\Delta NDII_{previous\ typhoon}$ of each typhoon pair using bootstrapped comparisons on means as $\Delta NDII_{typhoon} - \Delta NDII_{previous\ typhoon}$ over 5000 iterations. A positive 95% confidence interval (95% CI) indicates greater canopy damage for the target typhoon than for the preceding typhoon. Then, for both the annual and the biennial cases, we grouped studied typhoons into two groups describing the scenarios, where either a weaker target typhoon followed a stronger typhoon (wind $speed_{typhoon}$ < wind $speed_{previous\ typhoon}$, stronger-then-weaker scenario) or a stronger target typhoon followed a weaker typhoon (wind $speed_{typhoon}$ > wind $speed_{previous\ typhoon}$, weaker-then-stronger scenario). Here, the maximum wind speed was the mean maximum wind speed across all pixels. The two groups were compared using bootstrapped comparisons of means (5000 iterations) comparing the ΔNDII of the stronger-then-weaker typhoon scenario to ΔNDII of the

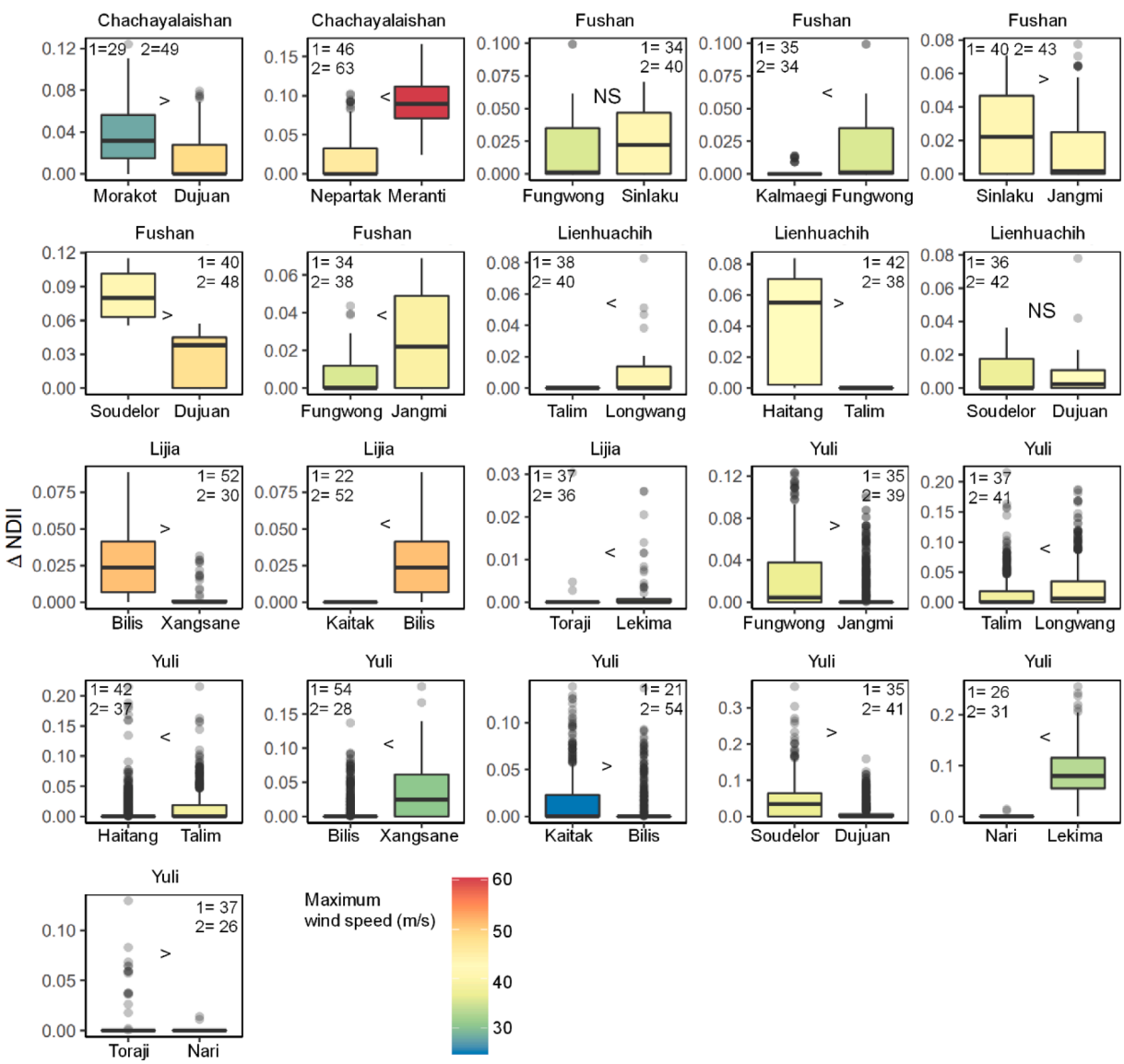

Fig. 2. Relative NDII change (ΔNDII) measured following two consecutive typhoons occurring within the same year. The maximum wind speed (meter per second) measured for each typhoon is shown in color and indicated for the preceding (1) and target typhoon (2) in each panel. Significant differences are detected using bootstrapped comparisons on means (Supplementary Material Table S3) and they are indicated with the symbols above each pair of boxplot, with > indicating significantly greater damage during the preceding typhoon (95% confidence interval < 0), < indicating significantly greater damage during the following typhoon (95% confidence interval > 0). NS indicates the absence of significant difference (95% confidence interval includes 0).

weaker-then-stronger typhoon scenario. A positive 95% CI suggests that the target typhoons in the weaker-then-stronger scenario caused less damage than in the stronger-then-weaker scenario.

3. Results

3.1. Typhoon damage is predicted by the typhoon characteristics and recent typhoon disturbances

Typhoon-induced drops in NDII were detected in all sites (Figs. 2-3). Windwardness of target typhoon and the windwardness of the preceding typhoon had a correlation of 0.71 ($p < 0.001$) in the annual analysis and 0.16 in the biennial analysis ($p < 0.001$).

Predictors used in the models had low to moderate correlations for both the annual and the biennial analyses and therefore were not excluded ($\leq$0.42; Supplementary Material, Table S2). In the annual analysis, the linear mixed model had marginal R^2 of 0.40 and conditional R^2 of 0.61 (Table 1). ΔNDIIs (*i.e.*, canopy damage) were positively related with pre-cyclone NDII. The canopy change caused by previous typhoons had significant relationship with ΔNDII: ΔNDII decreased with increasing damage associated with the previous typhoon ($\Delta NDII_{previous\ typhoon}$; -0.002 ± 0.0004, Table 1). However, typhoon characteristics (wind speed, windwardness) did not have a significant role in explaining ΔNDII ($p \geq 0.11$).

In the biennial analysis, the model had a marginal R^2 of 0.12 and conditional R^2 of 0.29 (Table 1). Pre-disturbance NDII was positively related to typhoon-induced change, whereas ΔNDII associated with the past typhoon season was not significant ($p = 0.46$).

3.2. Forest canopy damage of successive typhoons

ΔNDII between successive typhoons was not always significantly different in both the annual and biennial analyses (Figs. 2-3). In the annual analysis, there was no trend for either greater (ten cases) or less

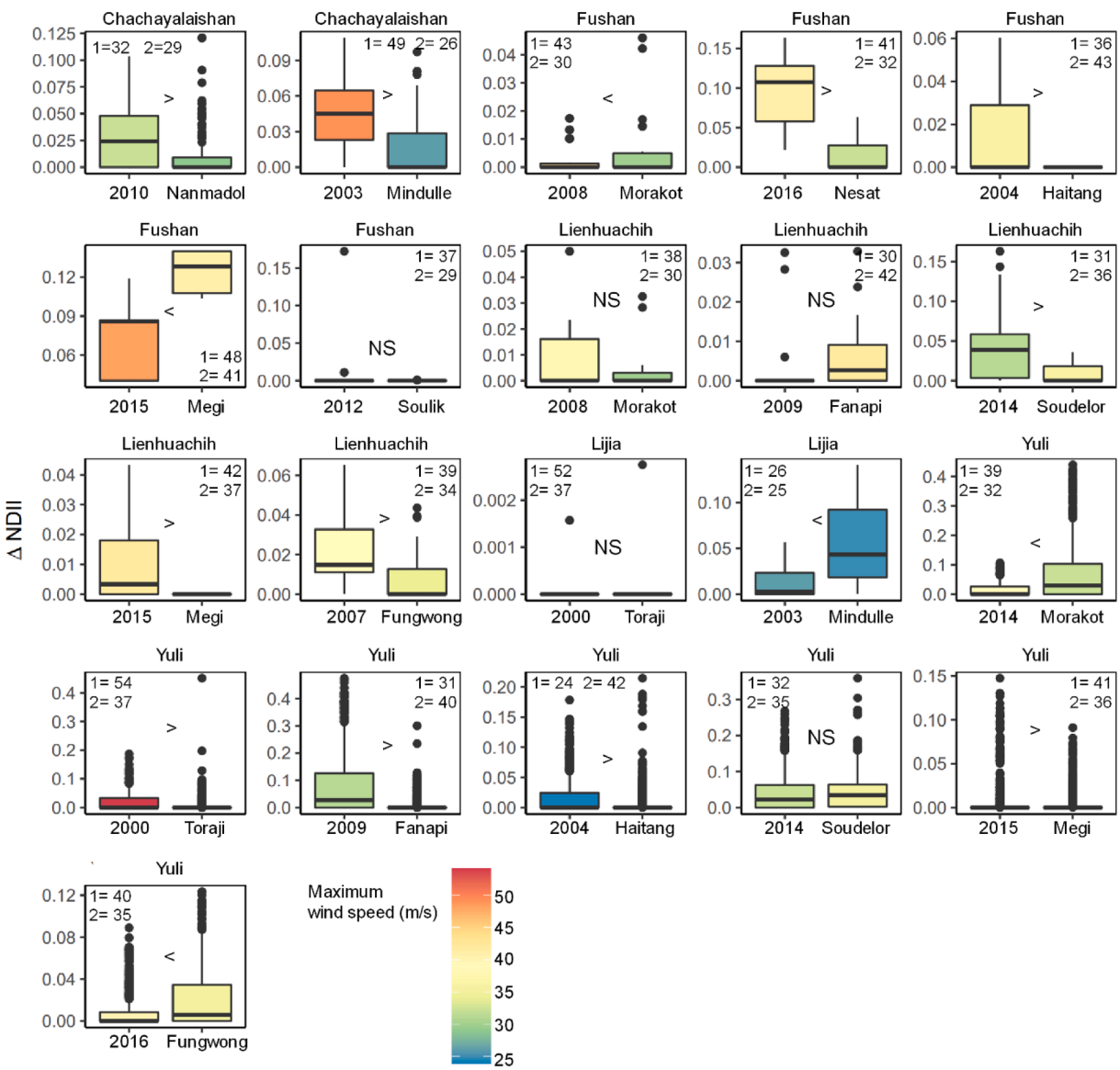

Fig. 3. Relative NDII change (ΔNDII) measured after the previous typhoon season (year) and the first typhoon of the second typhoon season (indicated by its name). The maximum wind speed (meter per second) measured for each typhoon is shown in color and indicated for the preceding season (1) and target typhoon (2) in each panel. Significant differences are detected using bootstrapped comparisons on means (Supplementary Material Table S3) and they are indicated with the symbols above each pair of boxplot, with > indicating significantly greater damage during the preceding typhoon season (95% confidence interval < 0), < indicating significantly greater damage during the following typhoon (95% confidence interval > 0). NS indicates the absence of significant difference (95% confidence interval includes 0).

Table 1
Linear mixed-effects model coefficients and statistics of the annual and biennial models. Coefficient means (with standard errors, SE) are given for the change in Normalized Difference Infrared Index (ΔNDII) caused by typhoons preceding a second typhoon during the same season (annual analysis) or the next season (biennial analysis). Note: ΔNDII response was log transformed, all fixed factors were centered and scaled with a mean of 0 and a standard deviation of 1 except for wind speed because for some events the wind speed was the same across all the pixels.

	Annual analysis			Biennial analysis		
Predictors	**Coefficient (SE)**	***t***	***p***	**Coefficient (SE)**	***t***	***p***
Intercept	0.141 (0.024)	5.980	<0.001	0.164 (0.044)	3.747	<0.001
Wind speed	0.001 (0.001)	1.582	0.114	−0.0002 (0.001)	−0.200	0.842
Windwardness	0.0001 (0.0003)	0.427	0.670	0.001 (0.0004)	1.173	0.241
$\Delta NDII_{previous\text{-}typhoon}$	−0.002 (0.0004)	−4.088	<0.001	0.001 (0.001)	0.735	0.462
elevation	−0.000003 (0.000002)	−1.562	0.118	−0.0002 (0.001)	−0.133	0.894
$NDII_{pre\text{-}typhoon}$	0.160 (0.006)	26.014	<0.001	0.144 (0.008)	17.985	<0.001
Statistics	$n = 6420$; df = 6394; AIC = − 35972.92; Marginal $R^2 = 0.402$; Conditional $R^2 = 0.611$; random effect variance = 0.0004			$n = 5893$; df = 5867; AIC = − 28278.82; Marginal $R^2 = 0.116$; Conditional $R^2 = 0.286$; random effect variance = 0.0004		

canopy (nine cases) damage associated with the second typhoon among the 21 pairs of typhoons studied (Fig. 2). However, in the biennial analysis, canopy damage caused by the second typhoon was generally less than the damage caused by the strongest typhoon of the preceding typhoon season: the preceding typhoon season had significantly higher damage 52% of the time (11 of 21 typhoon pairs versus five of 21 for the second typhoon) (Fig. 3).

Overall, the typhoon with the greater wind speed of each pair of typhoons tended to cause greater NDII reduction in both the annual and biennial analyses (Fig. 3 and Fig. 4). However, ten cases in the annual analysis (Fig. 3) and nine cases in the biennial analysis (Fig. 4), had greater NDII reduction associated with the weaker typhoon of the two (Fig. 3 and Fig. 4). Mean ΔNDII associated with the second typhoon was greater when the second typhoon had stronger wind speed than the preceding disturbance in the annual analysis (95 %CI − 0.004;−0.0004, 0.017 ± 0.0006 versus 0.020 ± 0.001), although the opposite was observed in the biennial analysis (95% CI 0.002;0.0070, 0.024 ± 0.0011 versus 0.019 ± 0.0007). However, there were six cases in the annual analysis and four cases in the biennial analysis in which ΔNDII was smaller for the second typhoon than for the first typhoon, even when the second typhoon had greater wind speed than the first.

4. Discussion

4.1. Damage detection

Studies of cyclone effects on forest canopies have often highlighted the effect of strong winds and heavy rains on forest canopy damage through defoliation. Remote sensing-derived VIs, such as NDII, indirectly register canopy damage in tropical and subtropical forests by measuring reductions in canopy water content (*i.e.*, reflectance) (Peereman et al., 2020; Zhang et al., 2016; Schwartz et al., 2019). Notably, the changes detected using our method only represent short-term storm-related canopy damages, such as defoliation (de Beurs and Townsend, 2008), and not the delayed canopy mortality that can occur in the months after cyclone passage, which could represent a significant portion of total cyclone-induced tree mortality (Bellingham et al., 1995; Imbert et al., 1998). Additionally, the effect of early canopy recovery in our observations should be minor, because our analyses used images from a maximum of 30 days following cyclone events. Even though tropical forest canopies can regrow quickly (Ostertag et al., 2003), the majority of canopy recovery likely begins at one to two months after cyclone passage (Feng et al., 2020; Gang et al., 2020; Hu and Smith, 2018).

4.2. Current and past typhoon effects on canopy damage

As expected, the pre-disturbance canopy state was a significant predictor of typhoon-induced canopy damage because cyclone damages are related to the stand developmental state (Kim et al., 2020; Lin et al., 2020). Factors like tree size, canopy area, and LAI are key modulators of cyclone damage magnitude (Dittus, 1985; Hall et al., 2020; Harrington et al., 1997; Ostertag et al., 2005). Harrington et al. (1997) have reported similar positive relationships between cyclone-induced reductions of LAI and pre-disturbance LAI and tree height in a Hawaiian forest. In addition, Feng et al. (2020) showed that the Hurricane Maria induced damages increased with greater remotely-sensed pre-disturbance green vegetation (derived from spectral mixture analysis), and canopy height and forest age in Puerto Rico. Moreover, comparing multiple hurricanes, Feng et al. (2021) showed that pre-disturbance green vegetation remained among the most important predictors of hurricane-induced damages. Because the variation in NDII has been related to defoliation and changes in forest canopy biomass (Dahal et al., 2014; de Beurs and Townsend, 2008), we suggest that the higher wind drag associated with higher NDII values likely contribute to increased cyclone-driven forest damage (Lin et al., 2020).

However, unlike forest developmental state, typhoon characteristics were not significant in explaining the variation in canopy damage. It is likely that modelled wind speeds do not always accurately represent the actual wind conditions in the forests, because of the coarse spatial resolution of this study (*i.e.*, at the resolution of MODIS imagery), rough landscape topography, and dynamic wind fields (Boose et al., 1994; Negrón-Juárez et al., 2014b). Some tropical cyclones may have high wind speed but little rainfall, whereas others have high rainfall and weak winds (Cortés-Ramos et al., 2020; Feng et al., 2021). This likely explains the complexity in finding a common set of predictors in our models across several cyclones over the same region. These results are consistent with Feng et al. (2021) who modelled the effects of hurricanes in the North Atlantic, and found that the importance of wind and rain in explaining vegetation disturbance varied over different regions because of hurricane properties and topographical effects (McEwan et al., 2011).

We suggest that canopy damages did not scale with the maximum sustained wind speed computed using HURRECON in our models because of the complexity of sites topography and the sheltering effect caused by the Taiwan Central Mountain Range (3000 m, Lee et al., 2008; McEwan et al., 2011), although wind speed is generally higher near the cyclones' eye (Turton, 2008). In addition, we postulate that the lack of a relationship between windward aspect and typhoon wind direction may also arise from topographic effects (*e.g.*, topographic exposure, Boose et al., 1994), and the untested effect of cyclone track side, because wind speeds are generally greatest at the leading right quadrant of cyclone tracks in the northern hemisphere (Feng et al., 2020; Negrón-Juárez et al., 2014a). Windward landscape aspect of target and preceding typhoons in the annual analysis had a correlation of 0.71, implying that some areas are generally more exposed than others. Repeated exposure is likely a factor which increases forest resistance to cyclone damage as reported in other tropical forests (Feng et al., 2020; Peereman et al., 2022), but which may have a greater potential effect in Taiwan because of the high frequency of cyclones (Peereman et al., 2022). Increased resistance likely occurs via the removal of highly-susceptible tall trees or

those with large canopies, which results in reductions in forest stature over time, especially in frequently-disturbed expose areas (Lin et al., 2020), meaning that sheltered slopes can show smaller difference in damages than exposed slopes.

In addition to the expected role of pre-disturbance vegetation state (Hall et al., 2020; Lin et al., 2003; Taillie et al., 2020), our study demonstrates that the change in canopy cover caused by previous typhoons was a significant predictor of canopy damage caused by target typhoons. Although studies have related cyclone legacies to subsequent disturbances (Kim et al., 2020; Ostertag et al., 2005; Peereman et al., 2022), by using data across several forests from many typhoon seasons, our study provides evidence that disturbance legacies are an important part of forest dynamics in cyclone-prone areas (*e.g.*, Taiwan and the Caribbean). The significant negative role of past canopy cover reduction (*i.e.*, $\Delta NDII_{previous\ typhoon}$) in our model of the annual analysis implies that areas that were more-greatly disturbed in the same season are likely to be less-severely affected by a subsequent typhoon within that season. Even though tropical forest canopies can regrow quickly (Ostertag et al., 2003), the onset of recovery likely begins at one to two months after cyclone passage (Feng et al., 2020; Gang et al., 2020; Hu and Smith, 2018). Therefore, a possible explanation is that these forests have lost most of the vulnerable canopy surface area after the first typhoon of the season, and will experience lesser relative damage by the second typhoon due to reduced canopy surface areas.

Previous typhoons reduce the amount of vulnerable matter before the target typhoon occurs. This removal effect was found to be an important modulator of canopy damage in Puerto Rico, explaining the decrease in damage severity of Hurricane Georges (in 1998) relative to Hurricane Hugo (in 1989) (Ostertag et al., 2003). In Taiwan, residual effects were also observed. Canopy damage severity typically decreased for target typhoons in comparison with the preceding typhoon, even when the preceding typhoon was weaker than the target typhoon (Fig. 2). This could explain why forests in Taiwan, although frequently exposed to typhoons, persist and usually show less damage than forests of other regions in response to cyclones of similar intensity (Hogan et al., 2018; Lin et al., 2011; Peereman et al., 2022).

Multiple other unexamined factors probably play a role in explaining forest canopy damage to cyclones, given that our models marginal R^2 ranged between 0.12 for the biennial analysis and 0.40 for the annual analysis. Topography can be important in explaining cyclone damage variation across landscapes (McLaren et al., 2019). For example, some areas are more-repeatedly disturbed than others because of a higher exposure or stronger wind speeds (Boose et al., 1994; Boose et al., 2004; Feng et al., 2020; Negrón-Juárez et al., 2014a; Negrón-Juárez et al., 2014b; Zhang et al., 2013). Where possible more topographical variables (*e.g.*, terrain roughness) could potentially be included to improve the model fit.

4.3. The role of past typhoons changes between annual and biennial analyses

A unique finding of our study is that past typhoons had an increased role in explaining target typhoon disturbance if they occurred during the same season than if they occurred a season earlier. One possible reason is that by the next year forest canopy had recovered substantially through the budding and leafing in March and April (Lin et al., 1997). Rapid re-leafing means that there are fewer canopy disturbance legacies interacting with typhoons of the next season.

It is not surprising that the stronger of the two typhoons in each of the typhoon pairs generally caused greater canopy damage, as high winds are the key agent damaging tree canopies. However, it is interesting that the weaker-then-stronger scenario more frequently caused severe canopy damages in the annual analysis than in the biennial analysis, with six and three cases respectively (Figs. 2-3). Likely, canopies opened by a previous disturbance can be more exposed to wind gusts within the same year than they are one year later, once the canopy has started to recover (Inagaki et al., 2008; Leitold et al., 2021). However, the mechanisms leading to less canopy disturbances from subsequent cyclones may be different between the Pacific basin (*i.e.*, Taiwan) and the North Atlantic basin. In the North Atlantic basin (*i.e.*, the Caribbean) the decreases in disturbance severity caused by the second of two hurricanes were attributed to the lower amount of vulnerable canopy biomass (Kim et al., 2020; Ostertag et al., 2003). In contrast, the decreased damage severity from subsequent typhoons in our study seems to be related to less residual effects associated with higher canopy resistance (*i.e.*, decreased litterfall, Xu et al., 2004), as well as faster recovery and thus lower wind exposure. Further studies of the effects of multiple successive cyclones on canopy disturbance and recovery dynamics are necessary because the interactions between wind, rain and tree crowns are incredibly complex, often resulting in a highly variable and patchy damage signature across forest landscapes, and because cyclone return intervals are variable (Boose et al., 2004; Negrón-Juárez et al., 2014a; Negrón-Juárez et al., 2014b).

Our study clearly demonstrates that forest landscapes in Taiwan can rapidly overcome much of the residual effects of recent disturbances because canopy change induced by past typhoons is less important a year later than during the same typhoon season. However, residual effects of cyclones are likely different between Taiwan and regions with less frequent cyclone disturbance due to the differences in the magnitude and rate of recovery (*i.e.*, forest biomass increment) before the next disturbance event. The projected increase in cyclone intensity and number of landfall cyclones (Kossin et al., 2020; Wang and Toumi, 2021) may shape tropical forests in novel ways because of interactions between disturbances legacies from preceding cyclones and target storms are likely to change. Further research is needed to determine whether forests under very frequent cyclone disturbances (*e.g.*, those in the Northwestern Pacific) experience lower residual effects, and thus may be less threatened by cyclone intensification than other regions.

4.4. Vegetation indices and remote sensing of consecutive typhoon disturbances

Our use of NDII has uncovered forest canopy cover dynamics because NDII is related to canopy water content (Jin and Sader, 2005; Wang et al., 2010). Nevertheless, our analyses were limited by the frequent cloud cover associated with the typhoon season, which led to the exclusion of some satellite imagery. Clouds prevented the observation of additional consecutive disturbances in our analysis even though MODIS sensors provide images with a temporal resolution finer than one day. For landscape to regional studies, geostationary satellites with very fine temporal resolution, such as Himawari 8 (Hashimoto et al., 2021; Khan et al., 2021), and the use of solar-induced fluorescence as well as drone- and LiDAR-based methods such as GEDI (Dubayah et al., 2020) may help to explore the effects of future cyclones on forest canopies (Duan et al., 2017; Gang et al., 2020; Leitold et al., 2021; Miura and Nagai, 2020).

5. Conclusions

Typhoon-mediated disturbances of Taiwanese forests between 2001 and 2017 shows that canopy damage (as seen through ΔNDIIs) is, in part, explained by the pre-disturbance vegetation state ($NDII_{pre\text{-}typhoon}$), but also by the canopy change associated with the preceding typhoon ($\Delta NDII_{previous\ typhoon}$). The negative relationship between past typhoon-induced canopy change and target typhoon damage invalidated our hypothesis regarding damage facilitation, as damage by a second typhoon within one year decreased when preceding typhoons had already caused the significant canopy disturbance. Yet, within a single typhoon season, the second of two typhoons can sometimes result in greater canopy damage when it had higher wind speed. Thus, we conclude that for Taiwanese forests, the interactive disturbance effects on canopy damage dynamics usually diminish by the next typhoon season. As a result, low typhoon residual effects may be one factor which

explain the relatively high levels canopy resistance to typhoon disturbance of Taiwanese forests. Further research is still required, however, to make firm generalizations about the relationships between successive disturbances to tropical forest canopies globally, or among different cyclone basins.

CRediT authorship contribution statement

Jonathan Peereman: Conceptualization, Methodology, Software, Formal analysis, Investigation, Data curation, Visualization, Writing – original draft. **J. Aaron Hogan:** Conceptualization, Methodology, Resources, Writing – review & editing. **Teng-Chiu Lin:** Conceptualization, Methodology, Investigation, Resources, Writing – review & editing, Supervision, Funding acquisition.

Declaration of Competing Interest

The authors declare that they have no known competing financial interests or personal relationships that could have appeared to influence the work reported in this paper.

Acknowledgments

We thank Dr. Chung-Te Chang (Adam) for providing the shapefiles of the Fushan and Lienhuachih reserves. We acknowledge the use of MODIS data, which are a NASA product. This research is supported by the Ministry of Science and Technology (grant numbers 108-2313-B-003 -001 -MY3, 110-2811-B-003 -502). We thank Dr. Christopher Patrick, William McDowell and John Kominoski for organizing the Ecosystem Responses to Hurricanes Synthesis Workshop funded by National Science Foundation (NSF) workshop grant no. DEB no 1903760 which facilitated the collaboration among the authors of this study.

Appendix A. Supplementary material

Supplementary data to this article can be found online at https://doi.org/10.1016/j.foreco.2022.120430.

References

Asner, G.P., 2001. Cloud cover in Landsat observations of the Brazilian Amazon. Int. J. Remote Sens. 22 (18), 3855–3862. https://doi.org/10.1080/01431160010006926.

Bellingham, P.J., Kapos, V., Varty, N., Healey, J.R., Tanner, E.V.J., Kelly, D.L., Dalling, J. W., Burns, L.S., Lee, D., Sidrak, G., 1992. Hurricanes need not cause high mortality: the effects of Hurricane Gilbert on forests in Jamaica. J. Trop. Ecol. 8 (2), 217–223. https://doi.org/10.1017/S0266467400006386.

Bellingham, P.J., Tanner, E.V.J., Healey, J.R., 1995. Damage and responsiveness of Jamaican montane tree species after disturbance by a hurricane. Ecology 76 (8), 2562–2580. https://doi.org/10.2307/2265828.

Boose, E.R., Foster, D.R., Fluet, M., 1994. Hurricane impacts to tropical and temperate forest landscapes. Ecol. Monogr. 64 (4), 369–400. https://doi.org/10.2307/2937142.

Boose, E.R., Serrano, M.I., Foster, D.R., 2004. Landscape and regional impacts of hurricanes in Puerto Rico. Ecol. Monogr. 74 (2), 335–352. https://doi.org/10.1890/02-4057.

Brokaw, N.V.L., Grear, J.S., 1991. Forest structure before and after Hurricane Hugo at three elevations in the Luquillo Mountains. Puerto Rico. Biotropica 23 (4), 386–392. https://doi.org/10.2307/2388256.

Buma, B., Wessman, C.A., 2011. Disturbance interactions can impact resilience mechanisms of forests. Ecosphere 2 (5), 1–13. https://doi.org/10.1890/ES11-00038.1.

Burslem, D.F.R.P., Whitmore, T.C., 1999. Species diversity, susceptibility to disturbance and tree population dynamics in tropical rain forest. J. Veg. Sci. 10 (6), 767–776. https://doi.org/10.2307/3237301.

Busetto, L., Ranghetti, L., 2016. MODIStsp: an R package for preprocessing of MODIS Land Products time series. Computers & Geosciences 97, 40–48. https://doi.org/10.1016/j.cageo.2016.08.020.

Cameron, C., Maharaj, A., Kennedy, B., Tuiwawa, S., Goldwater, N., Soapi, K., Lovelock, C.E., 2021. Landcover change in mangroves of Fiji: Implications for climate change mitigation and adaptation in the Pacific. Environmental Challenges 2, 100018. https://doi.org/10.1016/j.envc.2020.100018.

Ceccato, P., Flasse, S., Tarantola, S., Jacquemoud, S., Grégoire, J.-M., 2001. Detecting vegetation leaf water content using reflectance in the optical domain. Remote Sens. Environ. 77 (1), 22–33. https://doi.org/10.1016/S0034-4257(01)00191-2.

Chambers, J.Q., Fisher, J.I., Zeng, H., Chapman, E.L., Baker, D.B., Hurtt, G.C., 2007. Hurricane Katrina's Carbon Footprint on U.S. Gulf Coast Forests. Science 318 (5853). https://doi.org/10.1126/science.1148913.

Cortés-Ramos, J., Farfán, L.M., Herrera-Cervantes, H., 2020. Assessment of tropical cyclone damage on dry forests using multispectral remote sensing: The case of Baja California Sur. Mexico. J. Arid Environ. 178, 104171 https://doi.org/10.1016/j.jaridenv.2020.104171.

Dahal, D., Liu, S., Oeding, J., 2014. The Carbon Cycle and Hurricanes in the United States between 1900 and 2011. Sci. Rep. 4 (1), 5197. https://doi.org/10.1038/srep05197.

de Beurs, K.M., McThompson, N.S., Owsley, B.C., Henebry, G.M., 2019. Hurricane damage detection on four major Caribbean islands. Remote Sens. Environ. 229, 1–13. https://doi.org/10.1016/j.rse.2019.04.028.

de Beurs, K.M., Townsend, P.A., 2008. Estimating the effect of gypsy moth defoliation using MODIS. Remote Sens. Environ. 112 (10), 3983–3990. https://doi.org/10.1016/j.rse.2008.07.008.

de Gouvenain, R.C., Silander, J.A., 2003. Do tropical storm regimes influence the structure of tropical lowland rain forests? Biotropica 35 (2), 166–180. https://doi.org/10.1111/j.1744-7429.2003.tb00276.x.

Dittus, W.P. J., 1985. The influence of cyclones on the dry Evergreen forest of Sri Lanka. Biotropica 17 (1), 1–14. https://doi.org/10.2307/2388371.

Duan, F., Wan, Y., Deng, L., 2017. A novel approach for coarse-to-fine windthrown tree extraction based on unmanned aerial vehicle images. Remote Sens. 9 (4), 306. https://doi.org/10.3390/rs9040306.

Dubayah, R., Blair, J.B., Goetz, S., Fatoyinbo, L., Hansen, M., Healey, S., Hofton, M., Hurtt, G., Kellner, J., Luthcke, S., Armston, J., Tang, H., Duncanson, L., Hancock, S., Jantz, P., Marselis, S., Patterson, P.L., Qi, W., Silva, C., 2020. The Global Ecosystem Dynamics Investigation: High-resolution laser ranging of the Earth's forests and topography. Science of Remote Sensing 1, 100002. https://doi.org/10.1016/j.srs.2020.100002.

Feng, Y., Negrón-Juárez, R.I., Chambers, J.Q., 2020. Remote sensing and statistical analysis of the effects of Hurricane María on the forests of Puerto Rico. Remote Sens. Environ. 247, 111940 https://doi.org/10.1016/j.rse.2020.111940.

Feng, Y., Negrón-Juárez, R.I., Chambers, J.Q., 2021. Multi-cyclone analysis and machine learning model implications of cyclone effects on forests. Int. J. Appl. Earth Obs. Geoinf. 103, 102528 https://doi.org/10.1016/j.jag.2021.102528.

Flynn, D.F.B., Uriarte, M., Crk, T., Pascarella, J.B., Zimmerman, J.K., Aide, T.M., Ortiz, M.A.C., 2010. Hurricane disturbance alters secondary forest recovery in Puerto Rico. Biotropica 42 (2), 149–157. https://doi.org/10.1111/j.1744-7429.2009.00581.

Frolking, S., Palace, M.W., Clark, D.B., Chambers, J.Q., Shugart, H.H., Hurtt, G.C., 2009. Forest disturbance and recovery: a general review in the context of spaceborne remote sensing of impacts on aboveground biomass and canopy structure. J. Geophys. Res. Biogeosci. 114, G00E02. https://doi.org/10.1029/2008jg000911.

Gang, C., Pan, S., Tian, H., Wang, Z., Xu, R., Bian, Z., Pan, N., Yao, Y., Shi, H., 2020. Satellite observations of forest resilience to hurricanes along the northern Gulf of Mexico. For. Ecol. Manage. 472, 118243 https://doi.org/10.1016/j.foreco.2020.118243.

Gao, B.-C., 1996. NDWI—A normalized difference water index for remote sensing of vegetation liquid water from space. Remote Sens. Environ. 58 (3), 257–266. https://doi.org/10.1016/S0034-4257(96)00067-3.

Hall, J., Muscarella, R., Quebbeman, A., Arellano, G., Thompson, J., Zimmerman, J.K., Uriarte, M., 2020. Hurricane-induced rainfall is a stronger predictor of tropical forest damage in Puerto Rico than maximum wind speeds. Sci. Rep. 10, 4318. https://doi.org/10.1038/s41598-020-61164-2.

Hardisky, M.A., Klemas, V., Smart, R.M., 1983. The influence of soil salinity, growth form, and leaf moisture on the spectral reflectance of *Spartina alterniflora* canopies. Photogramm. Eng. Remote Sensing 49 (1), 77–83.

Harrington, R., A., Fownes, J.H., Scowcroft, P.G., Vann, C.S., 1997. Impact of Hurricane Iniki on native Hawaiian *Acacia koa* forests: damage and two-year recovery. J. Trop. Ecol., 13(4): 539-558. 10.1017/S0266467400010701.

Hashimoto, H., Wang, W., Dungan, J.L., Li, S., Michaelis, A.R., Takenaka, H., Higuchi, A., Myneni, R.B., Nemani, R.R., 2021. New generation geostationary satellite observations support seasonality in greenness of the Amazon evergreen forests. Nat. Commun. 12 (1), 684. https://doi.org/10.1038/s41467-021-20994-y.

Hijmans, R.J., 2019. raster: Geographic data analysis and modeling.

Hogan, J.A., Feagin, R.A., Starr, G., Ross, M., Lin, T.-C., O'connell, C., Huff, T.P., Stauffer, B.A., Robinson, K.L., Lara, M.C., Xue, J., Reese, B.K., Geist, S.J., Whitman, E.R., Douglas, S., Congdon, V.M., Reustle, J.W., Smith, R.S., Lagomasino, D., Strickland, B.A., Wilson, S.S., Proffitt, C.E., Hogan, J.D., Branoff, B. L., Armitage, A.R., Rush, S.A., Santos, R.O., Campos-Cerqueira, M., Montagna, P.A., Erisman, B., Walker, L., Silver, W.L., Crowl, T.A., Wetz, M., Hall, N., Zou, X., Pennings, S.C., Wang, L.-J., Chang, C.-T., Leon, M., Mcdowell, W.H., Kominoski, J.S., Patrick, C.J., 2020. A Research Framework to Integrate Cross-Ecosystem Responses to Tropical Cyclones. Bioscience 70 (6), 477–489. https://doi.org/10.1093/biosci/biaa034.

Hogan, J.A., Zimmerman, J.K., Thompson, J., Uriarte, M., Swenson, N.G., Condit, R., Hubbell, S., Johnson, D.J., Sun, I.F., Chang-Yang, C.-H., Su, S.-H., Ong, P., Rodriguez, L., Monoy, C.C., Yap, S., Davies, S.J., 2018. The frequency of cyclonic wind storms shapes tropical forest dynamism and functional trait dispersion. Forests 9 (7), 404. https://doi.org/10.3390/f9070404.

Hu, T., Smith, R.B., 2018. The impact of Hurricane Maria on the vegetation of Dominica and Puerto Rico using multispectral remote sensing. Remote Sens. 10 (6) https://doi.org/10.3390/rs10060827.

Ibanez, T., Keppel, G., Menkes, C., Gillespie, T.W., Lengaigne, M., Mangeas, M., Rivas-Torres, G., Birnbaum, P., 2019. Globally consistent impact of tropical cyclones on the

structure of tropical and subtropical forests. J. Ecol. 107 (1), 279–292. https://doi.org/10.1111/1365-2745.13039.
Imbert, D., Roustéau, A., Labbé, P., 1998. Ouragans et diversité biologique dans les forêts tropicales. L'exemple de la Guadeloupe. Acta Oecol. 19 (3), 251–262. https://doi.org/10.1016/S1146-609X(98)80029-5.
Inagaki, Y., Kuramoto, S., Torii, A., Shinomiya, Y., Fukata, H., 2008. Effects of thinning on leaf-fall and leaf-litter nitrogen concentration in hinoki cypress (*Chamaecyparis obtusa* Endlicher) plantation stands in Japan. For. Ecol. Manage. 255 (5–6), 1859–1867. https://doi.org/10.1016/j.foreco.2007.12.007.
IUCN, UNEP-WCMC, 2021. The World Database on Protected Areas (WDPA) [On-line], [07/2021], Cambridge, UK: UNEP-WCMC. Available at: www.protectedplanet.net.
Janda, P., Ukhvatkina, O.N., Vozmishcheva, A.S., Omelko, A.M., Doležal, J., Krestov, P. V., Zhmerenetsky, A.A., Song, J.-S., Altman, J., 2021. Tree canopy accession strategy changes along the latitudinal gradient of temperate Northeast Asia. Global Ecol. Biogeogr. 30 (3), 738–748. https://doi.org/10.1111/geb.13259.
Jin, S., Sader, S.A., 2005. Comparison of time series tasseled cap wetness and the normalized difference moisture index in detecting forest disturbances. Remote Sens. Environ. 94 (3), 364–372. https://doi.org/10.1016/j.rse.2004.10.012.
Johnstone, J.F., Allen, C.D., Franklin, J.F., Frelich, L.E., Harvey, B.J., Higuera, P.E., Mack, M.C., Meentemeyer, R.K., Metz, M.R., Perry, G.L., Schoennagel, T., Turner, M. G., 2016. Changing disturbance regimes, ecological memory, and forest resilience. Front. Ecol. Environ. 14 (7), 369–378. https://doi.org/10.1002/fee.1311.
Khan, A.M., Stoy, P.C., Douglas, J.T., Anderson, M., Diak, G., Otkin, J.A., Hain, C., Rehbein, E.M., McCorkel, J., 2021. Reviews and syntheses: Ongoing and emerging opportunities to improve environmental science using observations from the Advanced Baseline Imager on the Geostationary Operational Environmental Satellites. Biogeosciences 18 (13), 4117–4141. https://doi.org/10.5194/bg-18-4117-2021.
Kim, D., Millington, A.C., Lafon, C.W., 2020. Disturbance after disturbance: Combined effects of two successive hurricanes on forest community structure. Ann. Am. Assoc. Geogr. 110 (3), 571–585. https://doi.org/10.1080/24694452.2019.1654844.
Knapp, K.R., Diamond, H.J., Kossin, J.P., Kruk, M.C., Schreck, C.J., 2018. International Best Track Archive for Climate Stewardship (IBTrACS) Project, Version 4. [IBTrACS. EP.list.v04r00]. NOAA National Centers for Environmental Information.
Knapp, K.R., Kruk, M.C., Levinson, D.H., Diamond, H.J., Neumann, C.J., 2010. The International Best Track Archive for Climate Stewardship (IBTrACS): Unifying tropical cyclone best track data. B. Am. Meteorol. Soc. 91 (3), 363–376. https://doi.org/10.1175/2009BAMS2755.1.
Kossin, J.P., Knapp, K.R., Olander, T.L., Velden, C.S., 2020. Global increase in major tropical cyclone exceedance probability over the past four decades. Proc. Natl. Acad. Sci. USA 117 (22), 11975–11980. https://doi.org/10.1073/pnas.1920849117.
Lagomasino, D., Fatoyinbo, T., Castañeda-Moya, E., Cook, B.D., Montesano, P.M., Neigh, C.S.R., Corp, L.A., Ott, L.E., Chavez, S., Morton, D.C., 2021. Storm surge and ponding explain mangrove dieback in southwest Florida following Hurricane Irma. Nat. Commun. 12 (1), 4003. https://doi.org/10.1038/s41467-021-24253-y.
Lee, M.-F., Lin, T.-C., Vadeboncoeur, M.A., Hwong, J.-L., 2008. Remote sensing assessment of forest damage in relation to the 1996 strong Typhoon Herb at Lienhuachi Experimental Forest. Taiwan. For. Ecol. Manage. 255 (8–9), 3297–3306. https://doi.org/10.1016/j.foreco.2008.02.010.
Leitold, V., Morton, D.C., Martinuzzi, S., Paynter, I., Uriarte, M., Keller, M., Ferraz, A., Cook, B.D., Corp, L.A., González, G., 2021. Tracking the rates and mechanisms of canopy damage and recovery following Hurricane Maria using multitemporal Lidar data. Ecosystems. https://doi.org/10.1007/s10021-021-00688-8.
Li, Y., Mwangi, B., Zhou, S., Liu, S., Zhang, Q., Liu, J., Chu, G., Tang, X., Zhang, D., Wei, S., Lie, Z., Wu, T., Wang, C., Yang, G., Meng, Z., 2021. Effects of Typhoon Mangkhut on a monsoon evergreen broad-leaved forest community in Dinghushan Nature Reserve, lower subtropical China. Front. Ecol. Evol. 9 (333) https://doi.org/10.3389/fevo.2021.692155.
Lin, K.-C., Hamburg, S.P., Tang, S.-L., Hsia, Y.-J., Lin, T.-C., 2003. Typhoon effects on litterfall in a subtropical forest. Can. J. For. Res. 33 (11), 2184–2192. https://doi.org/10.1139/x03-154.
Lin, K.-C., Hamburg, S.P., Wang, L., Duh, C.-T., Huang, C.-M., Chang, C.-T., Lin, T.-C., 2017. Impacts of increasing typhoons on the structure and function of a subtropical forest: reflections of a changing climate. Sci. Rep. 7 (1), 4911. https://doi.org/10.1038/s41598-017-05288-y.
Lin, K.-C., Hwanwu, C.-B., Liu, C.-C., 1997. Phenology of broadleaf tree species in the Fushan Experimental Forest of northeastern Taiwan. Taiwan J. For. Sci. 12 (3), 347–355. https://doi.org/10.7075/TJFS.199709.0347.
Lin, T.-C., Hamburg, S.P., Lin, K.-C., Wang, L.-J., Chang, C.-T., Hsia, Y.-J., Vadeboncoeur, M.A., Mabry McMullen, C.M., Liu, C.-P., 2011. Typhoon disturbance and forest dynamics: lessons from a Northwest Pacific subtropical forest. Ecosystems 14 (1), 127–143. https://doi.org/10.1007/s10021-010-9399-1.
Lin, T.-C., Hogan, J.A., Chang, C.-T., 2020. Tropical cyclone ecology: a scale-link perspective. Trends Ecol. Evol. 7 (35), 594–604. https://doi.org/10.1016/j.tree.2020.02.012.
Liu, K.S., Chan, J.C.L., 2020. Recent increase in extreme intensity of tropical cyclones making landfall in South China. Clim. Dyn. 55 (5), 1059–1074. https://doi.org/10.1007/s00382-020-05311-5.
Liu, X., Zeng, X., Zou, X., González, G., Wang, C., Yang, S., 2018. Litterfall production prior to and during Hurricanes Irma and Maria in four Puerto Rican forests. Forests 9 (6), 367. https://doi.org/10.3390/f9060367.
Lugo, A.E., 2008. Visible and invisible effects of hurricanes on forest ecosystems: an international review. Austral Ecol. 33 (4), 368–398. https://doi.org/10.1111/j.1442-9993.2008.01894.x.
Lyapustin, A., Martonchik, J., Wang, Y., Laszlo, I., Korkin, S., 2011a. Multiangle implementation of atmospheric correction (MAIAC): 1. Radiative transfer basis and look-up tables. J. Geophys. Res. Atmos. 116 (D3) https://doi.org/10.1029/2010JD014985.
Lyapustin, A., Wang, Y., 2018. MCD19A1 MODIS/Terra+Aqua Land Surface BRF Daily L2G Global 500m and 1km SIN Grid V006. NASA EOSDIS Land Processes DAAC.
Lyapustin, A., Wang, Y., Laszlo, I., Kahn, R., Korkin, S., Remer, L., Levy, R., Reid, J.S., 2011b. Multiangle implementation of atmospheric correction (MAIAC): 2. Aerosol algorithm. J. Geophys. Res. Atmos. 116 (D3) https://doi.org/10.1029/2010JD014986.
Mabry, C.M., Hamburg, S.P., Lin, T.-C., Horng, F.-W., King, H.-B., Hsia, Y.-J., 1998. Typhoon disturbance and stand-level damage patterns at a subtropical forest in Taiwan. Biotropica 30 (2), 238–250. https://doi.org/10.1111/j.1744-7429.1998.tb00058.x.
McEwan, R.W., Lin, Y.-C., Sun, I.-F., Hsieh, C.-F., Su, S.-H., Chang, L.-W., Song, G.-Z.-M., Wang, H.-H., Hwong, J.-L., Lin, K.-C., Yang, K.-C., Chiang, J.-M., 2011. Topographic and biotic regulation of aboveground carbon storage in subtropical broad-leaved forests of Taiwan. For. Ecol. Manage. 262 (9), 1817–1825. https://doi.org/10.1016/j.foreco.2011.07.028.
McLaren, K., Denneko, L., Tanner, E., Bellingham, P.J., Healey, J.R., 2019. Reconstructing the effects of hurricanes over 155 years on the structure and diversity of trees in two tropical montane rainforests in Jamaica. Agr. Forest Meteorol. 276–277, 107621 https://doi.org/10.1016/j.agrformet.2019.107621.
Miura, T., Nagai, S., 2020. Landslide detection with Himawari-8 geostationary satellite data: A case study of a torrential rain event in Kyushu. Japan. Remote Sens. 12 (11), 1734. https://doi.org/10.3390/rs12111734.
Morimoto, J., Aiba, M., Furukawa, F., Mishima, Y., Yoshimura, N., Nayak, S., Takemi, T., Chihiro, H., Matsui, T., Nakamura, F., 2021. Risk assessment of forest disturbance by typhoons with heavy precipitation in northern Japan. For. Ecol. Manage. 479, 118521 https://doi.org/10.1016/j.foreco.2020.118521.
Murphy, H.T., Metcalfe, D.J., Bradford, M.G., Ford, A.J., 2014. Community divergence in a tropical forest following a severe cyclone. Austral Ecol. 39 (6), 696–709. https://doi.org/10.1111/aec.12133.
Nakagawa, S., Johnson, P.C.D., Schielzeth, H., 2017. The coefficient of determination R2 and intra-class correlation coefficient from generalized linear mixed-effects models revisited and expanded. J. R. Soc. Interface 14 (134), 20170213. https://doi.org/10.1098/rsif.2017.0213.
Negrón-Juárez, R., Baker, D.B., Chambers, J.Q., Hurtt, G.C., Goosem, S., 2014a. Multi-scale sensitivty of Landsat and MODIS to forest disturbance associated with tropical cyclones. Remote Sens. Environ. 140, 679–689. https://doi.org/10.1016/j.rse.2013.09.028.
Negrón-Juárez, R.I., Chambers, J.Q., Hurtt, G.C., Annane, B., Cocke, S., Powell, M., Stott, M., Goosem, S., Metcalfe, D.J., Saatchi, S.S., 2014b. Remote sensing assessment of forest disturbance across complex mountainous terrain: The pattern and severity of impacts of Tropical Cyclone Yasi on Australian rainforests. Remote Sens. 6 (6), 5633–5649. https://doi.org/10.3390/rs6065633.
Nunes, M.H., Both, S., Bongalov, B., Brelsford, C., Khoury, S., Burslem, D.F.R.P., Philipson, C., Majalap, N., Riutta, T., Coomes, D.A., Cutler, M.E.J., 2019. Changes in leaf functional traits of rainforest canopy trees associated with an El Niño event in Borneo. Environ. Res. Lett. 14 (8), 085005 https://doi.org/10.1088/1748-9326/ab2eae.
Ostertag, R., Scatena, F.N., Silver, W.L., 2003. Forest floor decomposition following hurricane litter inputs in several Puerto Rican forests. Ecosystems 6 (3), 261–273. https://doi.org/10.1007/PL00021512.
Ostertag, R., Silver, W.L., Lugo, A.E., 2005. Factors affecting mortality and resistance to damage following hurricanes in a rehabilitated subtropical moist forest. Biotropica 37 (1), 16–24. https://doi.org/10.1111/j.1744-7429.2005.04052.x.
Parker, G., Martínez-Yrízar, A., Álvarez-Yépiz, J.C., Maass, M., Araiza, S., 2018. Effects of hurricane disturbance on a tropical dry forest canopy in western Mexico. For. Ecol. Manage. 426, 39–52. https://doi.org/10.1016/j.foreco.2017.11.037.
Patricola, C.M., Wehner, M.F., 2018. Anthropogenic influences on major tropical cyclone events. Nature 563 (7731), 339–346. https://doi.org/10.1038/s41586-018-0673-2.
Peereman, J., Hogan, J.A., Lin, T.-C., 2020. Assessing typhoon-induced canopy damage using vegetation indices in the Fushan Experimental Forest. Taiwan. Remote Sens. 12 (10), 1654. https://doi.org/10.3390/rs12101654.
Peereman, J., Hogan, J.A., Lin, T.-C., 2022. Disturbance frequency, intensity and forest structure modulate cyclone-induced changes in mangrove forest canopy cover. Global Ecol. Biogeogr. 31, 37–50. https://doi.org/10.1111/geb.13407.
Ploton, P., Mortier, F., Réjou-Méchain, M., Barbier, N., Picard, N., Rossi, V., Dormann, C., Cornu, G., Viennois, G., Bayol, N., Lyapustin, A., Gourlet-Fleury, S., Pélissier, R., 2020. Spatial validation reveals poor predictive performance of large-scale ecological mapping models. Nat. Commun. 11 (1), 4540. https://doi.org/10.1038/s41467-020-18321-y.
R Core Team, 2020. R: A language and environment for statistical computing. R Foundation for Statistical Computing, Vienna, Austria.
Rossi, E., Rogan, J., Schneider, L., 2013. Mapping forest damage in northern Nicaragua after Hurricane Felix (2007) using MODIS enhanced vegetation index data. GIsci. Remote Sens. 50 (4), 385–399. https://doi.org/10.1080/15481603.2013.820066.
Roth, L.C., 1992. Hurricanes and mangrove regeneration: effects of Hurricane Joan, October 1988, on the vegetation of Isla del Venado, Bluefields. Nicaragua. Biotropica 24 (3), 375–384. https://doi.org/10.2307/2388607.
Schwartz, Naomi B., Budsock, Andrew B., Uriarte, María, 2019. Fragmentation, forest structure, and topography modulate impacts of drought in a tropical forest landscape. Ecology 100 (6), e02677. https://doi.org/10.1002/ecy.2677.
Sharma, A., Ojha, S.K., Dimov, L.D., Vogel, J.G., Nowak, J., 2021. Long-term effects of catastrophic wind on southern US coastal forests: Lessons from a major hurricane. PLoS One 16 (1), e0243362. https://doi.org/10.1371/journal.pone.0243362.

Simard, M., Romme, W.H., Griffin, J.M., Turner, M.G., 2011. Do mountain pine beetle outbreaks change the probability of active crown fire in lodgepole pine forests? Ecol. Monogr. 81 (1), 3–24. https://doi.org/10.1890/10-1176.1.

Simpson, R.H., Riehl, H., 1981. The hurricane and its impact. Louisiana State University Press., Baton Rouge, LA, 398 pp.

Sun, Y., Zhong, Z., Li, T., Yi, L., Hu, Y., Wan, H., Chen, H., Liao, Q., Ma, C., Li, Q., 2017. Impact of ocean warming on tropical cyclone size and its destructiveness. Sci. Rep. 7 (1), 8154. https://doi.org/10.1038/s41598-017-08533-6.

Taillie, P.J., Roman-Cuesta, R., Lagomasino, D., Cifuentes-Jara, M., Fatoyinbo, T., Ott, L. E., Poulter, B., 2020. Widespread mangrove damage resulting from the 2017 Atlantic mega hurricane season. Environ. Res. Lett. 15 (6), 064010 https://doi.org/10.1088/1748-9326/ab82cf.

Takemi, T., 2019. Impacts of global warming on extreme rainfall of a slow-moving typhoon: A case study for Typhoon Talas (2011). SOLA 15, 125–131. https://doi.org/10.2151/sola.2019-023.

Taylor, A.R., Dracup, E., MacLean, D.A., Boulanger, Y., Endicott, S., 2019. Forest structure more important than topography in determining windthrow during Hurricane Juan in Canada's Acadian Forest. For. Ecol. Manage. 434, 255–263. https://doi.org/10.1016/j.foreco.2018.12.026.

Thies, B., Groos, A., Schulz, M., Li, C.-F., Chang, S.-C., Bendix, J., 2015. Frequency of low clouds in Taiwan retrieved from MODIS data and its relation to cloud forest occurrence. Remote Sens. 7 (10), 12986–13004. https://doi.org/10.3390/rs71012986.

Tukey, J.W., 1977. Exploratory data analysis (Vol. 2, pp. 131-160). Addison-Wesley, Reading, Massachusetts.

Turton, S.M., 2008. Landscape-scale impacts of Cyclone Larry on the forests of northeast Australia, including comparisons with previous cyclones impacting the region between 1858 and 2006. Austral Ecol. 33 (4), 409–416. https://doi.org/10.1111/j.1442-9993.2008.01896.x.

Uriarte, M., Canham, C.D., Thompson, J., Zimmerman, J.K., Murphy, L., Sabat, A.M., Fetcher, N., Haines, B.L., 2009. Natural disturbance and human land use as determinants of tropical forest dynamics: results from a forest simulator. Ecol. Monogr. 79 (3), 423–443. https://doi.org/10.1890/08-0707.1.

Wang, H.-C., Lin, K.-C., Huang, C.-Y., 2016. Temporal and spatial patterns of remotely sensed litterfall in tropical and subtropical forests of Taiwan. J. Geophys. Res. Biogeosci. 121 (2), 509–522. https://doi.org/10.1002/2015JG003113.

Wang, H.-C., Wang, S.-F., Lin, K.-C., Lee Shaner, P.-J., Lin, T.-C., 2013. Litterfall and element fluxes in a natural hardwood forest and a Chinese-fir plantation experiencing frequent typhoon disturbance in Central Taiwan. Biotropica 45 (5), 541–548. https://doi.org/10.1111/btp.12048.

Wang, L., Qu, J.J., Xiong, X., Hao, X., Xie, Y., Che, N., 2006. A new method for retrieving band 6 of aqua MODIS. IEEE Geosci. Remote. Sens. Lett. 3 (2), 267–270. https://doi.org/10.1109/LGRS.2006.869966.

Wang, S., Toumi, R., 2021. Recent migration of tropical cyclones toward coasts. Science 371 (6528), 514. https://doi.org/10.1126/science.abb9038.

Wang, W., Qu, J.J., Hao, X., Liu, Y., Stanturf, J.A., 2010. Post-hurricane forest damage assessment using satellite remote sensing. Agr. Forest Meteorol. 150 (1), 122–132. https://doi.org/10.1016/j.agrformet.2009.09.009.

Xiao, M., 2021. Change in the occurrence frequency of landfalling and non-landfalling tropical cyclones over the Northwest Pacific. J. Clim. 34, 3145. https://doi.org/10.1175/jcli-d-20-0647.1.

Xu, X., Hirata, E., Shibata, H., 2004. Effect of typhoon disturbance on fine litterfall and related nutrient input in a subtropical forest on Okinawa Island. Japan. Basic Appl. Ecol. 5 (3), 271–282. https://doi.org/10.1016/j.baae.2004.01.001.

Yamamoto, S.-I., 2000. Forest gap dynamics and tree regeneration. J. For. Res. 5 (4), 223–229. https://doi.org/10.1007/BF02767114.

Zhang, G., Murakami, H., Knutson, T.R., Mizuta, R., Yoshida, K., 2020. Tropical cyclone motion in a changing climate. Science. Advances 6 (17), eaaz7610. https://doi.org/10.1126/sciadv.aaz7610.

Zhang, K., Thapa, B., Ross, M., Gann, D., 2016. Remote sensing of seasonal changes and disturbances in mangrove forest: a case study from South Florida. Ecosphere 7 (6), e01366. https://doi.org/10.1002/ecs2.1366.

Zhang, X., Wang, Y., Jiang, H., Wang, X., 2013. Remote-sensing assessment of forest damage by Typhoon Saomai and its related factors at landscape scale. Int. J. Remote Sens. 34 (21), 7874–7886. https://doi.org/10.1080/01431161.2013.827344.